Molecular Catalysis xxx (xxxx) xxx–xxx

Contents lists available at ScienceDirect

Molecular Catalysis

journal homepage: www.elsevier.com/locate/mcat

Application of metal complexes as biomimetic catalysts on glycerol oxidation

Adrián Rodrigo Parodi[a,*], Carolina Merlo[b], Agostina Córdoba[c], Claudia Palopoli[d], Joaquín Ferreyra[d], Sandra Signorella[d], María Luján Ferreira[e], Ivana Magario[a]

[a] Instituto de Investigación en Ingeniería de Procesos y Química Aplicada IPQA (UNC-CONICET), Universidad Nacional de Córdoba, Facultad de Ciencias Exactas, Físicas y Naturales, Av. Velez Sarsfield 1611, X5016GCA, Ciudad Universitaria, Córdoba, Argentina

[b] Instituto Multidisciplinario de Biología Vegetal, CONICET, Universidad Nacional de Córdoba Córdoba, Av. Velez Sarsfield 1611, Argentina

[c] Centro de Investigación y Tecnología Química (CITeQ) CONICET-Universidad Tecnológica Nacional, Facultad Regional Córdoba. Cruz Roja esq. Maestro López, X5016GCA, Ciudad Universitaria, Córdoba, Argentina

[d] IQUIR (Instituto de Química Rosario), Consejo Nacional de Investigaciones Científicas y Técnicas (CONICET), Facultad de Ciencias Bioquímicas y Farmacéuticas, Universidad Nacional de Rosario, Suipacha 531, S2002LRK Rosario, Argentina

[e] PLAPIQUI-Universidad Nacional del Sur-CONICET, CCT Bahía Blanca, Camino La Carrindanga Km 7, CC 717, 8000, Bahía Blanca, Argentina

ARTICLE INFO

Keywords:
Glycerol oxidation
Biomimetic catalysis
Reaction mechanism
Metal complexes

ABSTRACT

Two biomimetic complexes were evaluated as catalysts in the H_2O_2 mediated oxidation of glycerol, namely a peroxidase mimetic Fe(III) protoporphyrin complex (hematin) and the superoxide-dismutase mimetic complex of Mn(III) with 1,3-bis(5-sulphonatesalycilidenamino) propane (MnL^-). Catalysis was targeted to glyceraldehyde since antimicrobial power was proved for it. Glyceraldehyde evolved at a higher rate than the uncatalyzed reaction only with hematin acid treated solutions and kinetics were typical of a radical mechanism. Nonetheless, glycerol conversions were low. H_2O_2 bleached hematin and the immobilization on a porous matrix could not prevent this. Meanwhile, the catalatic activity of hematin was high but its peroxidatic activity was inhibited at pH > 8. Thus, the coordination of hematin compound I to H_2O_2 over glycerol may be the preferred route with the accumulation of peroxy radicals, able to degrade the porphyrinic ring -with probable iron releasing- but also contributing to glycerol oxidation. On the other hand, a prompt decay with time of the catalatic and peroxidatic activities of MnL^- was observed, which was improved by the addition of dimethylsulfoxide (DMSO), dimethylformamide (DMF) or acetone to the basic buffer system. Finally, EPR spectroscopy of MnL^- supported the hypothesis of the formation of an inactive bis-oxo-bridged Mn(IV)Mn(IV) dimer upon addition of H_2O_2.

1. Introduction

Green chemistry promotes the replacement of catalysts based on precious metals for less toxic, more abundant and economic transition metals like Fe, Mn, Cu or Zn. These metals also exist as complexes in the active centre of key enzymes of many redox processes (peroxidases, catalases, cytochrome-oxidases, superoxide-dismutase, among others). There are many examples in the literature where metal complexes are used as homogenous or heterogenous catalysts in oxidation reactions, motivated not only by the design of a suitable catalyst, but also as functional model systems of metalloenzymes. The central metal and the nature of the ligand determine the catalytic reactivity and selectivity of these complexes [1].

Due to the increase of the production of biodiesel, based on sustainability politics for renewable resources utilization, glycerol as the main by-product is being supplied at levels much higher than demanded. For this reason, its accumulation starts being problematic for the economy of the process. Its oxidation constitutes a possible valorization route and it generates firstly glyceraldehyde (GA) and dihydroxyacetone (DHA). DHA is used in sunless tanning formulations, in camouflaging segmental psoriasis, vitiligo and piebald lesions. It also has been reported as antifungal against causative agents of dermatomycosis [2]. GA is a saturated dihydroxy-aldehyde and is used in the preparation of adhesives and polyesters, as cellulose modifier and in the tanning of leather. Both products may be further oxidized, producing several compounds like glyceric acid, hydroxypyruvic acid, tartronic

* Corresponding author.
E-mail addresses: parodiadrian@hotmail.com (A.R. Parodi), cmerlo@agro.unc.edu.ar (C. Merlo), acordoba@utn.frc.edu.ar (A. Córdoba), palopoli@iquir-conicet.gov.ar (C. Palopoli), ferreyra@iquir-conicet.gov.ar (J. Ferreyra), signorella@iquir-conicet.gov.ar (S. Signorella), mlferreira@plapiqui.edu.ar (M.L. Ferreira), ivana.magario@unc.edu.ar (I. Magario).

https://doi.org/10.1016/j.mcat.2018.11.007
Received 30 June 2018; Received in revised form 6 November 2018; Accepted 8 November 2018
2468-8231/

acid and mesoxalic acid, among others. Nowadays the market for last commodities has not been developed due to the high cost of its production although all of them constitute high value structures in fine chemistry [3].

Aldehydes are electrophilic carbonyl compounds with biocidal properties. Aldehydes, notably formaldehyde and glutaraldehyde, are known to possess powerful antimicrobial activity [4] and have been widely used as disinfectants for their activity against bacteria and their spores, viruses and fungi [5]. A study suggests that the toxicity of the aldehydes is greater than of the ketones and it may be related to the greater electrophilic power of aldehydes [6]. During the peroxidation of lipids, different lipophilic α, β-unsaturated 4-hydroxy-aldehydes are produced like 4-hydroxy-2-trans-hexenal (HHE), 4-hydroxy2-trans-octenal (HOE), 4-hydroxy-2-trans-nonenal (HNE) and 4-hydroxy-2-trans-decenal (HDE). They are of interest because of their reactivity with biomolecules and their toxicity [7]. Aldehydes have the ability to disrupt proteins by the formation of Schiff's bases [8]. Antimicrobial action of aldehydes seems to be mainly located in the cell surface due to a disturbance of membrane proteins functions [9,10]. The biocidal activity of aldehydes decreases with the carbon chain length and also depends on the presence or absence of unsaturated links, being the unsaturated aldehyde more active than the saturated homolog [11]. The median lethal dose (LD_{50}) for GA in rats is 2 g kg^{-1} and is considered as slightly to moderately toxic [12].

In the last years, efforts to obtain chemical, enzymatic or microbiological catalytic systems suitable for the selective oxidation of glycerol toward the desired product DHA have increased [13–15]. However, there are few reports that make use of metal complexes based on Fe, Mn or Cu [16,17]. Great attention was given to the study of supported metal catalysts that use O_2 for the oxidation of glycerol, especially of Au, Pd, Pt, but also others like Rh and Ag [18–23]. One of the greatest drawbacks of these catalyst is their tendency to O_2 poisoning when its partial pressure is high. O_2 is readily available, cheap and suitable as oxidizing agent, especially when the substrate is in gas phase and big amounts are to be processed [24]. However, the operative and equipment costs needed to handle pressurized gases are high. In addition, aerobic oxidations might lead to combustion and conversions are maintained low to avoid over-oxidation [25,26]. On the other hand, in the production of fine chemistry compounds (characterized by having many functional groups, high boiling points and limited thermal stability) reactions are carried out in liquid phase, volumes are lower, and the processes are usually discontinuous. In these cases, the use of H_2O_2 offers the advantages that its use is simple and the costs are lower than in the case of O_2.

A variety of metalloporphyrins were studied in different oxidation reactions with diverse oxidizing agents. A nice overview can be seen in Che and Huang [27]. For instance, several Fe(III) metalloporphyrins were tested in the oxidation of alkanes, using O_2 as oxidizing agent [28]. There have also been made studies using different Fe complexes on the oxidation of alcohols [29–31] and even on glycerol oxidation [32]. Hematin porcine, a natural iron protoporphyrin, mimics the active site of peroxidases, the heme group of which performs, among others, proton abstraction from reducing substrates after being activated by H_2O_2 through the formation of an intermediate high-valent iron(IV)-oxoporphyrin π-cation radical [33–35]. Hematin demonstrated to be effective in the oxidation of phenolic substrates [36]. On the other hand, MnL^-, a water soluble Mn complex of 1,3-bis(5-sulphonatesalycilidenamino)propane (L^{4-}) (Scheme 1), presents similarities to other mononuclear Mn-Schiff base complexes which have been reported as suitable catalysts for the oxidation of alcohols in the presence of a primary oxidant (e.g., alkyl hydro peroxides, H_2O_2 or O_2) [37–40] and can be used in aqueous media [41–43].

Catalase activity serves as indicative that a complexed metal is oxidized by H_2O_2, generating an intermediate oxidized form able of interacting with a second H_2O_2 molecule to yield O_2. On the other hand, in order to mimic a peroxidase activity, the coordination of that intermediate oxidized state of the metal complex to a reducing substrate is required. Therefore, these two activities are competitive. When H_2O_2 solutions are prepared in acetone, the formation of 2-hydroxy-2-hydroperoxypropane stimulates the gradual availability of the oxidant thus diminishing its decomposition catalyzed by the metal complex. [44,45].

On the other hand, peroxidase activity of a metal complex can be simply checked by the straightforward and well established 4-aminoantypirine/phenol test, in which a purple quinoneimide adduct, is built on phenoxy and 4-aminoantypirine radicals pairing [46]. The evolution of peaks at 330 nm and 510 nm in UV/visible spectra of a reacting system are used to identify the quinoneimide adduct.

Despite both O_2 and H_2O_2 are environmentally friendly since neither produce dangerous by-products, H_2O_2 was selected as the oxidizing agent. Hence, both metal complexes, hematin and MnL^-, were evaluated as catalysts for the oxidation of glycerol using H_2O_2 as oxidant. Indeed, primary glycerol oxidation toward glyceraldehyde and dihydroxyacetone was pursued since they were expected to possess some antimicrobial activity. Therefore, low temperature and low oxidant concentration were always applied in order to avoid glycerol over-oxidation. Metal complexes as homogeneous catalyst but also supported on a porous matrix were applied. Besides, antimicrobial activity of DHA and GA against common pathogen bacteria was evaluated in order to target the catalysis to a bioactive molecule. Since the role of the solvent is crucial for the formation of catalytic relevant intermediates, the peroxidatic activity of both metal complex was checked in different reaction media in order to improve catalytic efficiencies. Results are discussed and evidence is presented based on undesirable metal complex coordination with the oxidant.

2. Experimental

2.1. Materials

Hematin porcine (MM = 633.49), glyceraldehyde (GA) and N-Methyl-N-(trimethylsilyl) trifluoroacetamide (MSTFA) were purchased to Sigma Aldrich (San Luis, United States). The complex NaMnL (MM = 620) was synthetized according to Moreno et al. [47]. Phenol and 4-aminoantipyrine were obtained from Tetrahedron (Godoy Cruz, Argentina), glycerol and H_2O_2 were acquired at Cicarelli (Santa Fe, Argentina). Basic fuchsin was acquired from Anedra (Tigre, Argentina). Hematin was immobilized on porous polymethacrylate beads functionalized with hexamethilenamino groups Relizyme™ HA403/S, which were kindly donated by Resindion S.R.L (Binasco, Italy). All the other reagents used in this work were of analytical grade, except for borax (technical grade).

2.2. Methods

2.2.1. Microorganisms and culture methods

Antibacterial activity was tested against *Escherichia coli* (ATCC 25922), *Pseudomonas aeruginosa* (ATCC 27853) and *Staphylococcus aureus* (ATCC 25923). Bacteria were incubated in tubes containing Müeller–Hinton (MH) broth (Britannia) for 24 h at 37 °C. Then, the bacteria cell concentration required to reduce the resazurin was determined for each strain. For this, serial ten-fold dilutions of the overnight culture were prepared in MH broth with 0.15% w/v agar. Aliquots (150 µL) of the inocula were dispensed into a microplate containing 50 µL of sterile distilled water and 10 µL of resazurin solution (0.01% w/v), and incubated for 2 h at 37 °C. The appropriate dilution to work was considered as the last one unable to reduce resazurin (blue). Resazurin is a redox indicator that is blue in its oxidised form and pink in its reduced form. The colony forming unit (CFU) per mL of this dilution was confirmed by the plate-counting method on MH agar.

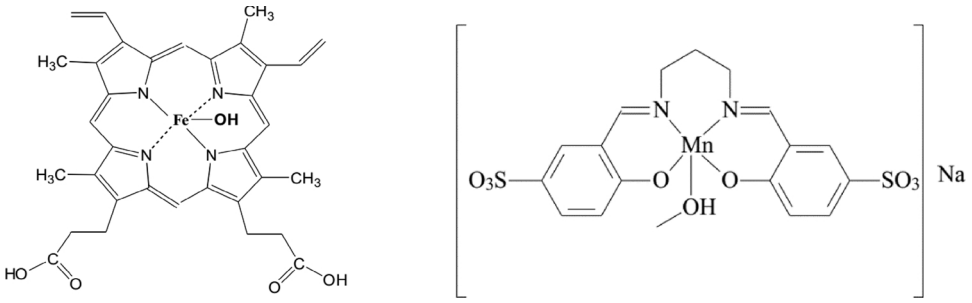

Scheme 1. Structures of complexes used in this work. Left: Hematin. Right: MnL^-.

2.2.2. Determination of the minimum inhibitory concentration (MIC) and minimum bactericidal concentration (MBC)

Serial twofold dilutions of GA, DHA and glycerol were prepared in sterile distilled water by vortexing it at room temperature. A sterile 96-well microplate was set up with the dilution of each bacteria as follows: column 1–10, 150 µL inoculum + 50 µL compound dilution; column 11, 150 µL inoculum + 50 of sterile distilled water (positive control = pink); column 12, 170 µL sterile assay medium (MH broth) + 50 of sterile distilled water (negative control = blue). Well contents were thoroughly mixed using a micropipette. Two trays were prepared for each strain and incubated at 37 °C for 24 h. After incubation, 10 µL of resazurin solution were added to all wells. After a second incubation of 2 h at 37 °C, wells were assessed visually for colour change, with the highest dilution remaining blue indicating the MIC [48]. The MBC was determined for the compounds that presented a MIC value. 200 µl of the dilution belonging to the MIC and the two previous dilutions were inoculated in MH agar and incubated at 37 °C for 24 h. The MBC was considered to be the last dilution that did not show cell growth.

2.2.3. Hematin immobilization

110 mg of hematin was dissolved in 100 mL of NaOH 0.01 M. Immobilization was carried out following two different protocols however, applied hematin/particles mass ratio was 54 mg/g in both cases. Covalent immobilization (Glu): 0.5 g of particles was incubated in 25 mL K_2HPO_4/NaOH pH 7 buffer 0.1 M containing (16.41 mM) glutaraldehyde under magnetic stirring at room temperature for 1 h. After that, the suspension was centrifugated for 5 min at 15,000 rpm. The particles were washed three times resuspending them in 25 mL buffer for one minute. The supernatant was withdrawn and discarded in every wash step. Modified particles obtained were incubated with 24 mL of hematin solution under magnetic stirring at room temperature for 2 h. Then, the suspension was centrifugated for 5 min at 15,000 rpm. The supernatant was recovered and diluted with distilled water into a 100-ml volumetric flask. The particles were washed three times resuspending them with 20 mL of distilled water and vortexed for 1 min. The supernatants were diluted to 25 mL and reserved. Supported hematin was then incubated with 25 mL Tris Buffer under magnetic stirring at room temperature for 1 h. Once again, the suspension was centrifugated and washed three times with distilled water. The supernatants were reserved. Electrostatic immobilization (D): 0.5 g of particles was incubated in 0.1 M acetate buffer pH 5 under magnetic stirring at room temperature for 18 h. After that, 50 mL of hematin solution was added to the suspension and incubated for 2 h. Precipitated hematin was observed so the pH was raised to 7 with NaOH 1 M and the suspension incubated for 19 h at room temperature. After that, the suspension was centrifugated for 5 min at 15,000 rpm. The supernatant was carefully withdrawn and recovered. The particles were washed three times resuspending them with 20 mL of buffer and vortex for 1 min.

The supernatants were used to estimate the amount of immobilized hematin. The absorbance of supernatants and wash waters were measured at 387 nm ($\varepsilon = 0.0469\ L\ mg^{-1}\ cm^{-1}$) and the amount of hematin attached to the support was calculated by means of a mass balance. A Perkin Elmer Lambda 35 spectrophotometer (Massachusetts, United States) was used for all the absorbance measurements. Thus, following parameters were calculated for both catalysts: the amount of attached hematin per gram of support (Qp) and the efficiency of immobilization, defined as the attached hematin respect to the initial amount of hematin in the solution. The values obtained for catalysts D and Glu were -respectively- Qp: 39 and 3.9 mg/g and efficiencies of immobilization of 74% and 5.9%.

Table 1
Conditions used in glycerol oxidation assays.

Exp.ID	Type of Catalyst	$C_{catalyst}$ (mM)	$C_{glycerol}$ (mM)	C_{H2O2} (mM)	H_2O_2 dosages	T (°C)	Solvent	$[Aldehyde]_{3\text{-}5\ h}$ or in Fig. (mM)
1	–	–	1000	138	1	35	Aqueous pH_0 5	5.2
2	–	–	1000	138	1	35	Aqueous pH_0 7	5.3
3	–	–	25	25	5*	35	Aqueous pH_0 5	Fig. 3
4	Free MnL^-	1.00	500	81	1	room	water	Fig. 1, right
5	Free MnL^-	1.00	500	81	1	room	MeCN/water 50:50	Fig. 1, right
6	Free hematin	0.16	1000	138	1	35	Aqueous pH_0 5	Fig. 1, left
7	Free hematin	0.16	1000	138	1	35	Aqueous pH_0 7	Fig. 1, left
8	Free hematin	0.16	1000	138	1	35	Aqueous pH_0 11	Fig. 1, left
9	Free hematin	0.16	100 - 1000	28 - 202	3*	35	Aqueous pH_0 5	Fig. 2, left
10	Free hematin	8 **	1000	100	5*	room	Buffer pH 5	Fig. 2, right
11	Supp hematin (Glu)	0.04	25	25	5*	35	Aqueous pH_0 5	2.0
12	Supp hematin (D)	0.04	25	25	5*	35	Aqueous pH_0 5	Fig. 3
13	$FeSO_4$	0.29	76	35	1	room	Aqueous pH_0 3.6	6.4
14	$FeSO_4$	0.66	76	70	5*	room	Aqueous pH_0 3.6	31

* Dosages at the beginning and after 1 h to give the reported applied concentration on the left.
** Dosages of 1.6 mM at 0, 1, 2, 3 and 4 h reaction time.

2.2.4. Glycerol oxidation assays

Hematin was dissolved in a NaOH 0.01 M aqueous solution and MnL^- was dissolved in distilled water to give mother solutions of 0.5–0.7 g/L and 31 g/L, respectively. Table 1 gives an overview of the conditions used in all glycerol oxidation assays. Reaction media were shaken and its temperature was maintained using a thermostatic bath. Reactions were initiated by the addition of H_2O_2. When applied, the following buffer solution was used: acetic acid/NaOH 0.1 M (pH 5). Otherwise, the initial pH was set by adding drops of 1 M HCl or NaOH to a glycerol aqueous solution. Samples of 200 µL were withdrawn at different time intervals and mixed with 800 µL of Schiff reagent. The last was prepared dissolving 1 g of basic fuchsin and 100 mL of 10% anhydrous sodium sulphite solution in 1 L distilled water prior to acidification with 10 mL of HCl. Schiff reagent lasts for two weeks in the dark [49]. Reaction samples were left to react for 30 min at room temperature and final absorbance was measured at 560 nm. The aldehyde concentration was calculated by means of a calibration curve. In the assay of highly concentrated free hematin (8 mM) samples were centrifuged before adding Schiff reagent. The interference of dissolved non-bleached hematin in this assay was corrected by deducing the absorbance at 560 nm after Schiff treatment of blank samples without glycerol.

2.2.5. Gas chromatography

A sample of the glycerol oxidation reaction media was withdrawn while stirring and centrifuged to eliminate the supported hematin. Next, 40 µL of the supernatant was withdrawn and dried at reduced pressure during 3 h to remove water. Pyridine was added, and the tube was vortexed for analytes re-dilution. A sample of this solution was placed in a second tube. Pyridine, n-hexanol as internal standard and N-Methyl-N-(trimethylsilyl) trifluoroacetamide (MSTFA) were added. The derivatization was carried out in an oil bath at 70 °C for 30 min. Derivatized samples were analysed using a Perkin Elmer Clarus 500 gas chromatograph equipped with a flame ionization detector (FID) and a PE elite-1 column of 15 m × 0.53 mm ID x 3 µm film thickness. A deactivated silica column of 5 m × 0.53 mm ID was used as a pre-column. All the injections were made on-column. Injector temperature program was as follows: 60 °C (1 min), increment at 15 °C/min until 230 °C (0 min) and then to 250 °C at a rate of 3 °C/min. Oven temperature program: 50 °C (1 min), increment of 15 °C/min until 210 °C (0 min), increment of 3 °C/min until 230 °C (0 min) increment of 15 °C/min until 240 °C (2 min), total run time 21 min. The temperature of the FID was set to 280 °C.

2.2.6. Catalatic activity test

The dissolved oxygen profile during the reaction was registered with an electrochemical Pasco Pasport sensor model PS-2108 (California, United States). The corresponding metal complex was dissolved in 5 mL of borate buffer 0.05 M pH 8.0 to give final concentrations of 2.1 and 0.044 mM for MnL^- and Hematin, respectively. The sensor was introduced and, under magnetic stirring at 100 rpm, the online measurement of dissolved O_2 was carried out using the software Pasco Capstone (trial version 1.8.0). After the stabilization of the signal, 57 µL of 30% W/V H_2O_2 (100 mM) were added and the measurement continued for at least 30 min.

2.2.7. Peroxidatic activity test

The influence of the solvent in the peroxidatic activity of metal complexes was evaluated through the phenol/4-aminoantipyrine/H_2O_2 reaction at room temperature in plastic cuvettes [46]. The reaction started by the one-time addition of H_2O_2, the cuvette was capped and inverted three times before being placed in the cup holder. Reaction conditions are shown in Table 2. The following solvents were tested: Borate buffer 0.05 M pH 8.0 and 50:50 mixtures of it with DMSO or acetone (set A and B of Table 2) and in 1:6 DMF:buffer phosphate of pH 7 (set C and D of Table 2). Influence of media pH on peroxidatic activity was also checked for hematin. Following 0.1 M buffer solutions were applied as solvents: Na/K phosphate for pH 6 and 7, Tris-HCl for pH 8 and 9 and carbonate for pH 10.0 and 10.8 (E of Table 2). Peroxidatic activity of supported hematin was also determined (set F of Table 2). Reaction samples were withdrawn at different time intervals while stirring and centrifugated for 5 min. The supernatant was taken and its absorbance measured. The catalityc activity is defined for supported hematin as (U/g_{solid}), where U stands for µmoles of quinoneimide aduct produced per minute. Unless specified, absorbance measurements were made at 510 nm.

Table 2
Conditions used in peroxidatic activity tests.

Set	C_{phenol} (mM)	$C_{4\text{-aminoantipyrine}}$ (mM)	C_{H2O2} (mM)	Catalyst	$C_{catalyst}$ (mM)	In Fig.
A	8.00	0.11	17	Free hematin	0.01	4
B	8.00	0.11	17	MnL^-	0.08	5
C	3.09	7.85	33	MnL^-	0.031	6
D	0.27	0.67	3.3	MnL^-	0.0027	6
E	8.00	0.11	15	Free hematin	0.09	5
F	8.00	0.11	4	Supp. hematin	0.016	–

2.2.8. EPR spectroscopy

EPR spectra were registered on a Bruker ESP 300 E spectrometer with a microwave frequency generated with a Bruker ER 04 (9–10 GHz). 6.6 mg of NaMnL were dissolved in 5 mL of DMSO. 1.5 mL of this solution were diluted with equal volume of borate buffer of pH 8, and 49 µL of phenol were added to this solution. 32 µL of H_2O_2 were added to 2 mL of the complex + phenol mixture in DMSO:borate buffer, and aliquots were frozen in liquid nitrogen at different time intervals.

3. Results and discussion

3.1. Antimicrobial activity of GA and DHA standard solutions

The antibacterial activity of GA, DHA and glycerol were investigated on *Escherichia coli, Pseudomonas aeruginosa* and *Staphylococcus aureus*. Only GA inhibited the evaluated strains and *E. coli* was the most susceptible (Table 3). DHA and glycerol did not show antibacterial activity against any of the analysed bacteria at the evaluated concentrations. Kajiwara et al. [50] detected bacteriostatic action on *E. coli* by different aliphatic unsaturated aldehydes at a concentration of 0.05 g/L, being 3Z-hexenal the most efficient. Citral also displayed moderate activity against gram positive and gram negative bacteria and the strains tested in this work were among them [4]. Matasyoh et al. [51] reported MIC values of 163 g/L and 108 g/L of *Coriandrum sativum* essential oil against *E. coli* and *S. aureus*, respectively. *P. aeruginosa* was resistant. This oil contained 56% aldehyde, mainly 2E-decenal and decanal. Monoterpenes with OH functional groups, commonly encountered in essential oils, present combined antimicrobial action against the strains tested in this work showing MIC

Table 3
Minimal inhibitory concentration (MIC) and minimal bactericidal concentration (MBC) of aqueous GA solutions. Range tested: 0.04–25 g/L.

Microorganism	MIC (g/L)			MBC (g/L)		
	1° run	2° run	Mean	1° run	2° run	Mean
E. coli	6.25	6.25	6.25	6.25	6.25	6.25
S. aureus	9.38	6.25	7.81	6.25	9.38	7.81
P. aeruginosa	9.38	6.25	7.81	9.38	6.25	7.81

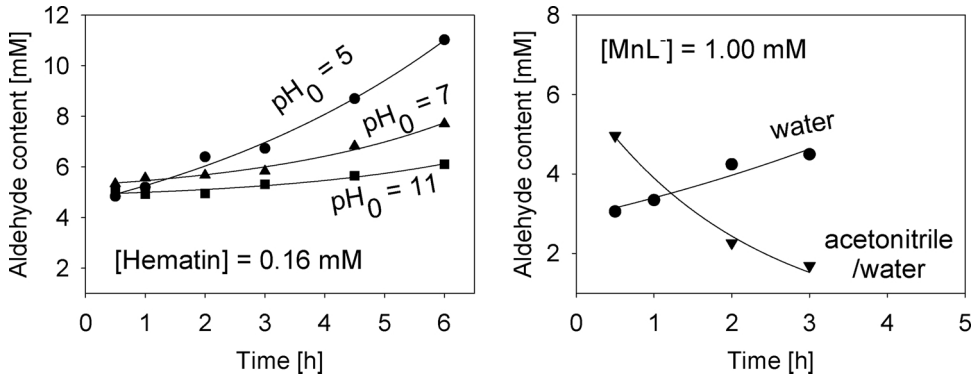

Fig. 1. Aldehyde evolution during metal complex/H_2O_2 treated glycerol aqueous solutions. Reaction conditions are indicated in Table 1.

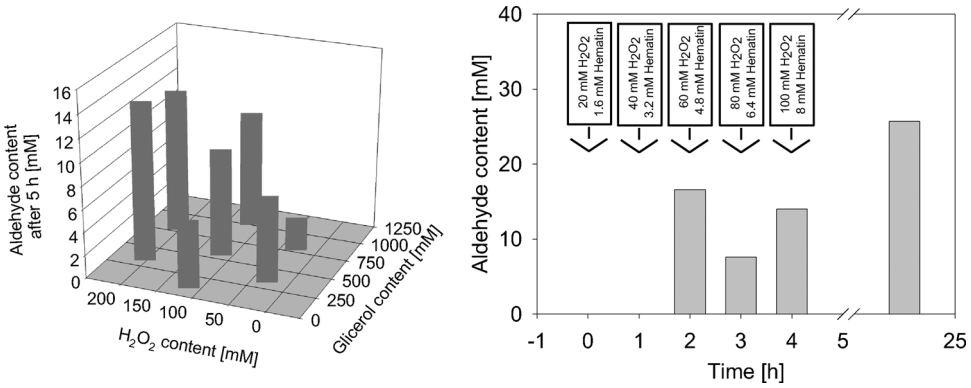

Fig. 2. Left: Aldehyde content after 5 h contact time of hematin/H_2O_2 treated glycerol solutions. Right: Aldehyde evolution of hematin treated buffered glycerol aqueous solution at pH = 5 during hematin/H_2O_2 stepwise addition. Reaction conditions in Table 1.

values in the wide range of 3.81–222 g/L [52]. MIC values of GA are low compared to those of synthetic antibiotics [53] however they fell inside the values of natural compounds as monoterpenes.

3.2. Glycerol oxidation with catalyst in solution

Hematin was tested as catalyst in aqueous media at different pH because its solubility increases with higher pH due to its carboxylate moieties. However, H_2O_2 tends to decompose at high pH values [54]. A variety of Mn(III) complexes are commonly used in acetonitrile as solvent [38] and the complex MnL^- is also soluble in water [47], hence it was tested in water and 1:1 water/acetonitrile mixtures. Fig. 1 shows aldehyde production during metal complex/H_2O_2 treated aqueous glycerol solutions in different solvents. Aldehyde content increased with contact time in the case of hematin although it was higher at lower pH. Crotti et al. [32] reported glycerol oxidation yielding DHA and formic acid as the only reaction products with conversions of up to 47% and selectivity towards DHA of up to 80% after 90 min using Fe complexes as homogeneous catalyst. The results here reported are quite different since the reactions were done in milder conditions (particularly, much less catalyst and H_2O_2 concentration).

On the other hand, aldehyde evolution in the MnL^-/H_2O_2 systems were up to 5 mM, which was equal to values measured in the absence of metal complex under similar reaction conditions (Table 1). Moreover, aldehyde decay was observed in the mixture acetonitrile/water as solvent. This result can be attributed to the over-oxidation of the aldehyde to the carboxylic acid such as observed for $[Cr(SO_3\text{-salen})]^+$ (salen = 1,2-bis(salicylidenamino)ethane) in 1:1 MeCN:H_2O [55] and immobilized $[Mn(SO_3\text{-salen})]^-$ in H_2O [56], which in the presence of H_2O_2 yielded low overall conversions of glycerol with the major product being formic acid. Unlike oxidation of glycerol, Mn(III)-Schiff base complexes proved to be efficient to catalyse the oxidation of primary and secondary alcohols to the corresponding carbonylic products using H_2O_2 as terminal oxidant, in MeCN [57], MeCN/H_2O [41] and ionic liquids [37]. Additionally, Shul'pin et al. [58] used a dinuclear Mn complex both in solution and immobilized and reported glycerol conversion of up to 45% and selectivity towards DHA of up to 15%. Glyceraldehyde was not obtained in those experiments.

No aldehyde evolved in blank trials of hematin/H_2O_2 solution in the absence of glycerol. The number of equivalents of produced GA was greater than applied hematin equivalents thus indicating that a catalytic cycle was present. In all hematin reaction trials, media turned from light brown to colorless with reaction time due to degradation of the Soret band of hematin [59]. The irreversible bleaching is consequence of the decrease of this band upon addition of H_2O_2 and it depends on the H_2O_2/hematin molar ratio. Probably, an inactivated form of hematin is built either by oxidation of the porphyrinic ring or by H_2O_2 promoted dimers formation [36]. Moreover, a green-brown precipitate appeared when the alkaline hematin mother solution was added to the glycerol solution adjusted to a pH of 5 and disappeared after 2 h contact time with H_2O_2 due to its degradation.

The effect of glycerol and H_2O_2 initial concentrations on aldehyde content was also evaluated after 5 h treatment with hematin. Selection of initial concentrations were made according to a Doehlert array [60] however, a response surface model could not be obtained since the standard error of the central point (26.9%) was higher than response variations. Results are summarized on Fig. 2 (left). Aldehyde content was higher at higher H_2O_2 initial concentrations in the range studied (28–202 mM). Glycerol concentration seems to be optimal at the central concentration around 500 mM. Nonetheless, aldehyde yields were low. The range of molar ratios employed were 186–1320 for H_2O_2/hematin and 0.04–1.15 for H_2O_2/glycerol. Although H_2O_2 was dosed in three stages (see Table 1) the intensity of the Soret band of hematin (395 nm) also decreased about 89 to 100% at the end of reaction in all cases.

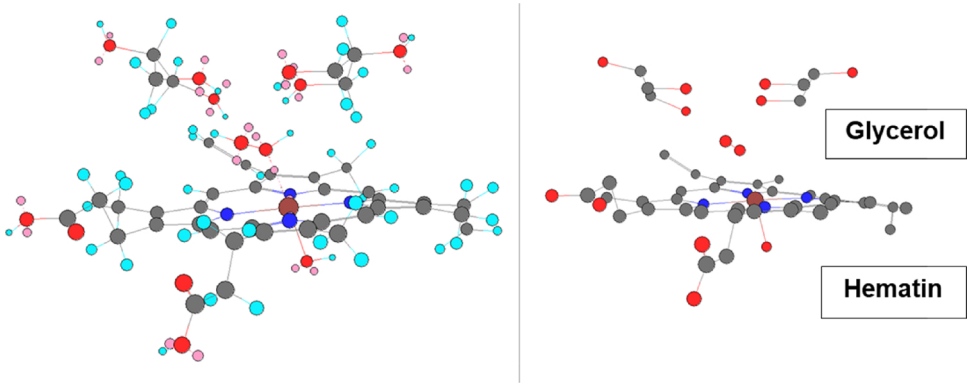

Scheme 2. Hydrogen peroxide coordinated to hematin and two glycerol molecules coordinated to hydrogen peroxide. Red: O, Grey: C Blue: N Pale blue: hydrogen pale pink: available orbitals for bonding.

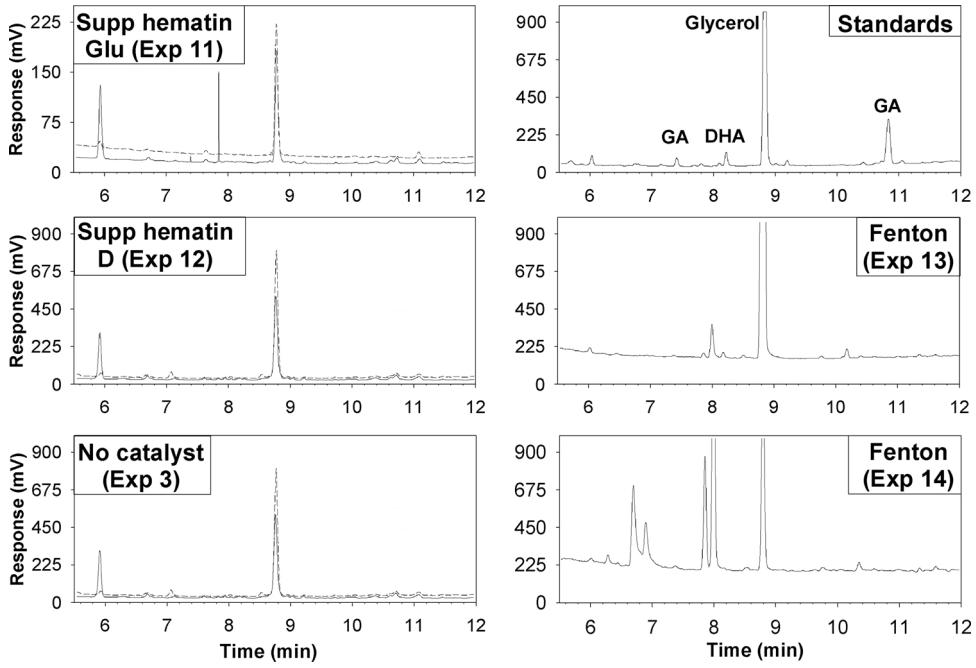

Fig. 3. Chromatograms of reaction media. Dashed line: at initial time, continuous line: after 6 h reaction. Fenton (Exp 13): after 3 h contact time. Fenton (Exp 14): after 24 h reaction time. See Table 1 for reaction conditions.

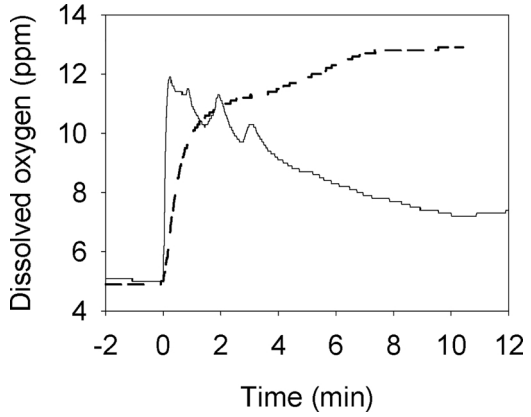

Fig. 4. Evolution of dissolved oxygen during MnL^{-}/ H_2O_2 (full line) and hematin/H_2O_2 (dotted line) solutions in borate buffer pH 8.0. At zero-time H_2O_2 was added. [MnL^{-}] = 2.1 mM. [Hematin] = 0.044 mM. $[H_2O_2]_0$ = 100 mM.

Therefore, an experimental run was conducted at a higher hematin concentration in order to prevent it from bleaching. In this run, H_2O_2/hematin molar ratio was equal to 66, but H_2O_2 and hematin were dosed in five stages at 0, 1, 2, 3 and 4 h (Table 1). Hematin bleaching was not observed; however, it remained insoluble and aldehyde evolution were in the order of those obtained with lesser amount of hematin (Fig. 2, right).

Hematin demonstrated to be a better catalyst to oxidize glycerol to GA at lower pH although being poorly soluble. The precipitation of hematin at a pH of 5 may prevent it from bleaching thus keeping it active for longer time. Another possible explanation is that iron is released from hematin and glycerol oxidation occurs through a Fenton-like reaction, which is only operative at low pH. Indeed, an acid glycerol solution treated with H_2O_2 in the presence of $FeSO_4$ showed GA production (see Table 1), which increases with the amount of iron applied. Farnetti et al. [17] observed glycerol oxidation, mainly to formic acid, catalyzed by ferrous and ferric chloride however under much higher content of iron and H_2O_2 than those applied in this work.

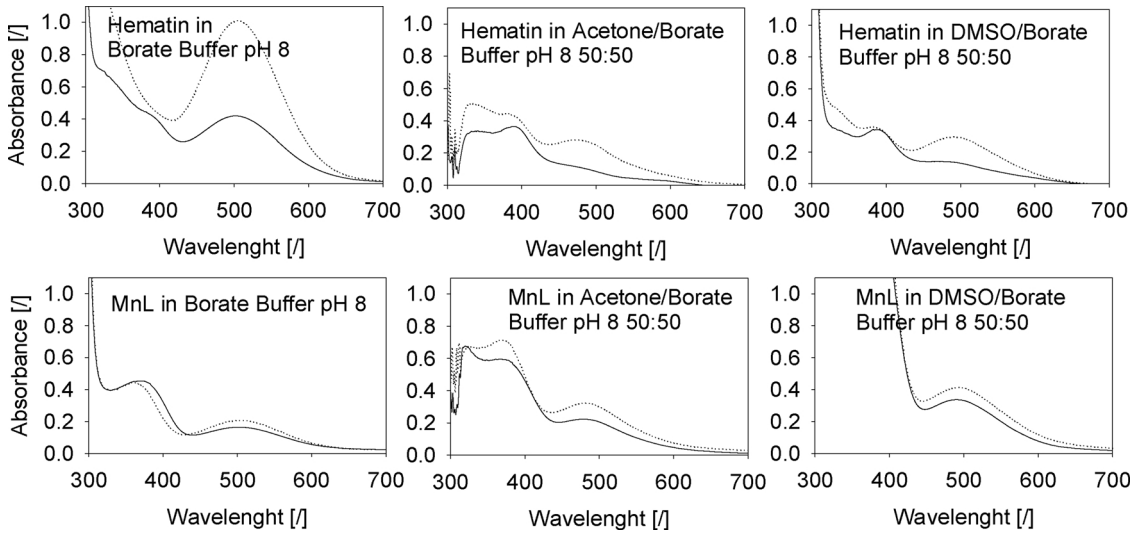

Fig. 5. UV/visible spectra of phenol/4-aminoantipyrine/H_2O_2 reaction systems at zero time (full lines) and at 10 min (dotted lines). See Table 2 for reaction conditions.

Table 4
Oxidation of phenol with H_2O_2 (and/or O_2) catalyzed by metal-Schiff base complexes.

Complex	r/[cat] (min^{-1})	Conditions	Reference
MnL^-	0.45	H_2O_2, 1:6 DMF:H_2O pH 7, 25 °C	This work
MnL_2^2	2.2	H_2O_2, pH 7, 35 °C	[64]
[Cu(acacen)]	3.1	H_2O_2, pH 7, 25 °C	[65]
$[Co(L^3)(N_3)_2]$	0.93	O_2, MeOH, 25 °C	[66]
CuL^4, CoL^4	0.15 – 0.20	1:1 O_2:H_2O_2, pH 6, 110 °C	[67]
FeL^5, CuL^5, ZnL^5, CoL^5, NiL^5	0.1 – 0.23	H_2O_2, MeCN, 70 °C	[68,69]
CoL^6	1.2 – 1.4	H_2O_2, miscellar solutions, 25 °C	[70]
CoL^7	0.14 - 0.19	O_2/H_2O_2, pH 6, 110 °C	[71]

L^2 = 1-hydroxy-5-[4-(2-hydroxybenzylideneamino)phenoxy]-3-oxapentane; acacen = acetylacetonateethylenediamine; L^3 = Schiff base condensation product of N,*N*-dimethyldipropylenetriamine and 3-ethoxysalicylaldehyde; L^4 = peripherally functionalized salicylaldimine dendrimers; L^5 = N,N'-bis(o-hydroxy acetophenone)ethylenediamine; L^6 = Schiff base ligands with morpholino or aza crown ether pendants; L^7 = N-(aryl)salicylaldimine.

Additional aspects have to be considered. First, glycerol, hydrogen peroxide and hematin can be involved in long range H-Bonding. This H-Bonding may hinder the reaction rate of the oxoperferryl π-cation radical Fe(IV) = O formation.

The Scheme 2 shows the lateral view of hydrogen peroxide coordinated to hematin with two glycerol molecules involved in an-extensive H bonding.

3.3. Glycerol oxidation with supported hematin

The fact that hematin is more efficient in GA production at lower pH implies the hindrance for providing the catalyst at higher concentrations in aqueous solutions because of the insolubility of hematin at pH lower than 7. Therefore, an attractive strategy for overcoming proper catalyst availability may be its immobilization on a solid matrix. Therefore, hematin was supported on a porous matrix and tested in the glycerol oxidation reaction. The peroxidatic activity of these batches yielded a catalytic activity of 9.78 and 1.55 U/g_{solid}, for catalyst D and Glu, respectively. Fig. 3 shows gas chromatogram of treated glycerol/H_2O_2 aqueous solutions with supported hematin and without catalyst. A chromatogram of a mixture of derivatized GA, DHA and glycerol standards is also presented for comparison. Peaks at 7.8 and 8.0 min corresponds to traces of a partial derivatized glycerol species.

Small peaks corresponding to GA (7.3 min and 10.8 min) arose only for catalyst Glu. However, a decrease on glycerol peak after 6 h related to initial time was observed in all cases. No other products were observed. The peak at 5.9 min corresponds to the internal standard, n-hexanol. Further attempts increasing the amount of supported hematin (1.7 mM) or H_2O_2 concentration (400 mM) did not yield higher glycerol conversion nor GA production (data not shown). Moreover, the solid support did not prevent hematin from bleaching, which always occurred at a rate dependent on the used H_2O_2 concentration. It has been reported in the literature glycerol conversions of up to 24.6% with a sulfonate-salen Fe(III) immobilized into Mg-Al layer double hydroxide (LDH) as catalyst and H_2O_2 as oxidant after four hours of reaction [56]. The main product was DHA and the selectivity towards GA was 4.2%.

Derivatized GA and DHA structures presented about 10% of the sensitivity of glycerol derivatized structure thus making its identification in reaction samples difficult. Therefore, gas chromatograms of glycerol treated solutions with Fenton reagent were also performed as a positive control since they gave the highest GA content according to the Schiff reagent. Small peaks at 7.3 min and 8.1 min arose due to the presence of GA and DHA, respectively (see Fig. 3). However, presence of peaks at 6.6, 6.8 and 6.3 min are also observed in the reaction media treated with higher $FeSO_4$ concentration and may account for other reaction products as *e.g.,* carboxylic acids derived from overoxidation of glycerol [17].

3.4. Catalatic and peroxidatic activities

Reaction systems of Figs. 1 and 2 always bubbled up when adding H_2O_2 to initiate the reaction especially at higher pH, most probably due to the catalase activity of hematin as a secondary reaction. Prior works by our group demonstrated oxygen evolution during hematin catalyzed oxidation of an antraquinone dye [36]. Fig. 4 shows the oxygen evolution with time during H_2O_2 treatment of catalyst solutions in aqueous

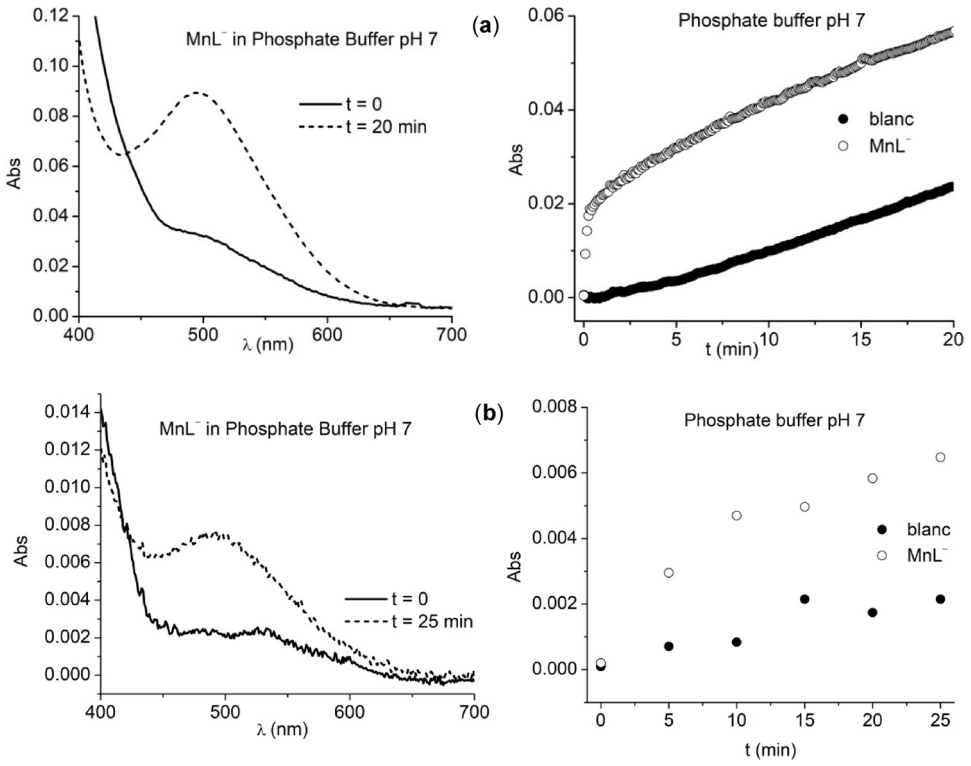

Fig. 6. Kinetics and UV/vis spectra of phenol/4-aminoantipyrine/H_2O_2 reaction system. Solvent: 1:6 DMF:Phosphate buffer pH 7. Measures of absorbance vs time were made at 496 nm. See Table 2 for reaction conditions.

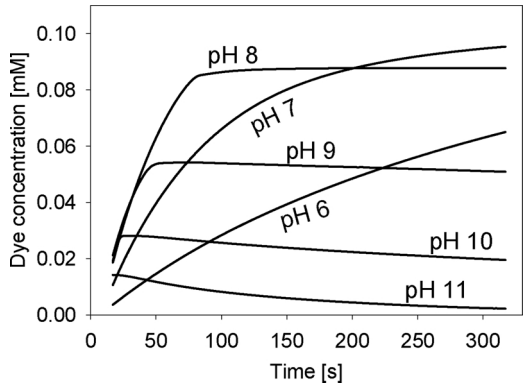

Fig. 7. Quinoneimide dye generation at different media pH during phenol/4-aminoantipyrine assay test (ε_{dye} = 13,473 M^{-1} cm^{-1}). See Table 2 for reaction conditions.

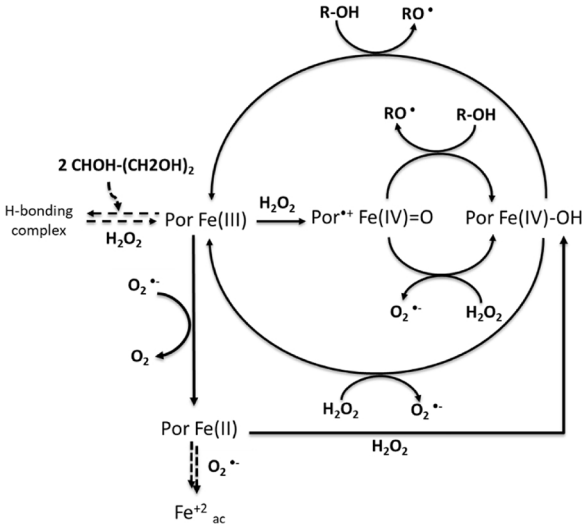

Scheme 3. Pseudocatalatic-peroxidatic mechanism proposed for the action of hematin on alcohols (ROH). Dotted lines denote new added routes. Por Fe(III) represents hematin ground state.

borate buffer of pH 8.0. The measured initial turnover rates were 1.04 and 8.71 mmol of H_2O_2 dismutation per min per mmol of catalyst, for MnL^- and hematin, respectively. These initial rates are in the range found for related mononuclear metal complexes [61]. In a prior work, a mechanism was proposed for interpreting H_2O_2 dismutation at alkaline pH in the presence of hematin [62] and included superoxide accumulation, which upon coordination to the resting state of hematin finally generates molecular oxygen.

In the case of MnL^- oxygen evolution was promptly stopped after the first few seconds; however, that evolution was sustained with time in the case of hematin. An inactivation process due to irreversible Mn oxidation may be present in case of MnL^-. As observed in Fig. 4, O_2 begins to decrease after 20 s. This O_2 consumption suggests that, in the basic conditions employed in this assay, the aerobic dimerization of MnL^- can be favored to yield a bis-oxo-bridged Mn(IV) dimer through the "reverse catalase reaction" as previously observed for a related Mn-salen complex [63].

Fig. 5 shows visible spectra of the aminoantipyrine/phenol reaction at the beginning of reaction and after 10 min. The high MnL amounts used interfered with the 300–400 nm region of the spectra, however a blank trial consisting of a MnL/H_2O_2 system (*i.e.* in the absence of phenol and 4-aminoantipyrine) revealed that no peak evolved at 510 nm indicating that it alone serves as indicative of quinoneimide formation. In the case of MnL^- a peak also evolved at 510 nm however the intensity reached after 10 min is low and similar to the one observed at the beginning of reaction. Therefore, MnL^- demonstrated some peroxidase activity that is stopped or inactivated at the beginning of reaction in the same manner as already observed in the case of its catalase activity. A remarkable improvement was obtained in the case

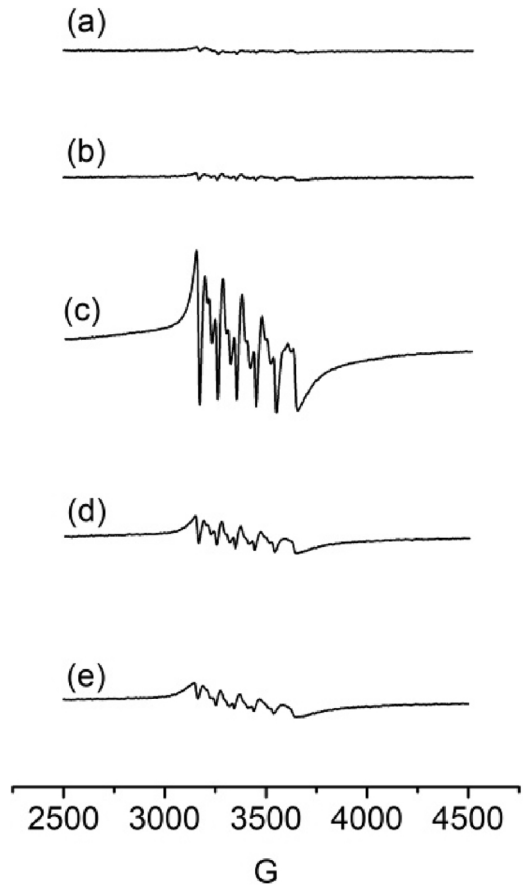

Fig. 8. Low temperature X-band EPR spectra of 1 mM MnL^- in DMSO (a); 1 mM MnL^- + 80 mM phenol in 50:50 DMSO:borate buffer (pH 8) before (b) and 35 s (c); 1 h (d); 1 day (e) after addition of 100 mM H_2O_2. ν = 9.52 GHz, T = 120 K, microwave power = 0.5 mW.

of MnL for both mixtures achieving up to a two-fold increase in activity by the addition of DMSO.

In a mixture of 1:6 DMF:phosphate buffer of pH 7, using 1:100:1000 catalyst:phenol:H_2O_2 ratio, MnL^- catalyzed the formation of the quinoneimide adduct with initial rate of 0.45 mmol of adduct per min per mmol of catalyst, 70-times faster than in the absence of the complex. The rate of catalytic phenol oxidation is within the range reported for other Schiff-base complexes (Table 4). After 2 min, this rate slowed and got closer to 0.2 μM min^{-1}, the rate of adduct formation from a mixture of phenol + 4-aminoantipyrine + H_2O_2, as shown in Fig. 6a. In this medium, the absorbance band of the adduct is centered at 496 nm and superimposes the peak of the complex [47]. Therefore, absorption of the starting complex was subtracted. A similar behavior was observed when 10-fold diluted solutions were employed (Fig. 6b). For the diluted mixture, the measured initial rate of formation of the dye was 0.03 mmol adduct per min per mmol of catalyst. After 20 min, the reaction slows down to 0.01 μM adduct per min and rate parallels the uncatalyzed reaction. The spectra of the adduct formed after 25 min of reaction and the starting complex are shown in Fig. 6b. When 1:1000:10,000 MnL^-: phenol: H_2O_2 ratios were used, addition of the complex did not show any catalytic effect on the reaction rate. Then, 1% of catalyst appears as the best proportion of the complex to catalyze phenol oxidation by H_2O_2. At higher proportion employed in basic medium (10% in borate buffer, pH 8) dimerization is favored and activity is lower.

MnL^- exists as a monomer in aqueous solution [47]. Solvents with higher donor numbers like DMSO and acetone, favor the formation of the high valent mononuclear Mn(IV) or Mn(V) complex involved in phenol oxidation. The formation of the oxidized mononuclear Mn(IV/V) complex competes with the aerobic dimerization of MnL^- in the basic medium that affords the bis-oxo-bridged Mn(IV) dimer [61]. This Mn(IV) dimer has no peroxidatic activity as shown by the absence of the absorption band at 510 nm in mixtures of phenol, 4-aminoantipyrine, H_2O_2 and an independently synthetized bis-oxo-bridged Mn(IV) dimer obtained following a reported method [72].

Quinoneimide formation catalyzed by hematin at neutral pH was already demonstrated in a prior work [46]. As suspected, hematin also showed peroxidase activity in borate buffer of pH 8. On the other hand, peroxidatic action was inhibited in these solvents' mixtures with hematin as catalyst. The dielectric constants of the applied mixtures of solvents are lower in comparison to aqueous solution, thus promoting homolytic cleavage of the O-O of H_2O_2 [73] however, according to the peroxidatic mechanism, an heterolytic cleavage is required to give the oxoperferryl π-cation radical Fe(IV)=O (i.e., mimicked compound I) responsible of the hydrogen abstraction of the phenol molecule [46]. Fig. 7 shows the evolution of the quinoneimide dye at different pH in hematin catalyzed systems. Initial rate of dye formation increased from pH 6 up to pH 8. However, end dye-values lowered with the increasing of pH indicating that reaction stopped sooner. Two possible routes may explain this finding: 1) hematin inactivation due to bleaching; or 2) hydrogen peroxide consumption due to its catalase action, both processes being favored at higher pH. Moreover, absorbance slowly decreased with time for pH values higher than 9, indicating dye degradation presumably by hydroxyl or superoxide radicals co-generated

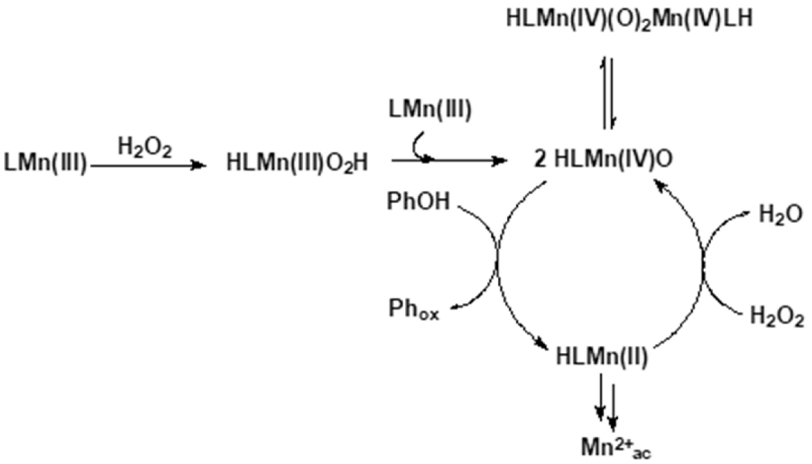

Scheme 4. Proposed mechanism for the competitive peroxidatic reaction and dimerization of MnL^-.

by the above mentioned processes. This finding is in accordance with the higher aldehyde production rate at lower pH values by the hematin/H_2O_2 treated glycerol solutions.

The pseudocatalatic-peroxidatic mechanism of hematin is represented in the Scheme 3. This mechanism was kinetically evaluated in a prior work by our group in the hematin-mediated oxidation of a phenolic dye but also in H_2O_2/hematin systems at alkaline pH [62]. Even at the lowest pH tested in this work the superoxide content was always higher than the hydroxy radicals. Dotted lines denote new routes added in order to interpret the evidence here presented with glycerol as the substrate. Thus, glycerol may not be a proper substrate for hematin compound I (Por•+ Fe(IV) = O) or hematin compound II (Por Fe(IV)-OH). Instead, reaction with a second molecule of hydrogen peroxide over glycerol coordination to hematin compound I may be the preferred route. This last coordination may generate superoxide radicals responsible for the observed hematin bleaching and finally iron releasing [59].

3.5. Electron paramagnetic resonance (EPR) spectroscopy of the MnL-complex

EPR was used to monitor the Mn oxidation state during the reaction of MnL^- with phenol in presence of H_2O_2. In the starting complex Mn (III) has an integer spin S = 2 and is silent in perpendicular mode X-band EPR spectroscopy [74]. On the other hand, any mononuclear Mn (II) (S = 5/2) or Mn(IV) (S = 3/2) formed in the reaction mixture can be detected by this technique. Also, mixed valence Mn(II)Mn(III) or Mn (III)Mn(IV) as well as Mn(II)Mn(II) dimers show characteristic multiline EPR signals and, if formed, can be easily detected [75]. On the contrary, oxo-bridged Mn(IV)Mn(IV) dimers exhibit strong antiferromagnetic exchange interactions, affording an EPR silent diamagnetic ground state (S = 0) with no contribution from excited states which are depopulated at low temperature. The 9.5 GHz band EPR spectrum of a frozen solution of MnL- in DMSO is shown in Fig. 8(a). This spectrum is essentially silent as expected for the Mn(III) complex. No spectral changes were observed after addition of 80 equivalents of phenol over the complex solution in DMSO/borate buffer (Fig. 8(b)) indicating the preservation of the Mn(III) center. Immediately after addition of 100 equiv. of H_2O_2 to the solution of MnL^-/phenol in DMSO/buffer, the EPR spectra exhibited an intense six-line signal at g ≈ 2 (hyperfine splitting of ≈ 90 G), with weak doublets inserted between the six absorptions (Δm = 1 nuclear-spin–forbidden transitions) characteristic of the hyperfine structure of an uncoupled Mn(II) ion (Fig. 8(c)). Interestingly, the intensity of this signal rapidly decreased and only a residual signal of an uncoupled Mn(II) species persisted at longer times (Fig. 8(d–e)), probably due to the release of Mn^{2+}_{aq} from the reduced form of the complex. These observations suggest that at short reaction times the peroxidatic activity of MnL^- could take place through a cycle involving Mn(IV)/Mn(II) active forms, which rapidly inactivate in agreement with the spectrophotometric results described above. The Mn^{2+}_{aq} content of the final mixture constitutes 10% of the starting MnL^- concentration; so most of the complex converts into an inactive EPR silent complex. The most probably candidate for this inactive species is an EPR silent bis-oxo-bridged Mn(IV)Mn(IV) dimer, the formation of which is favored in basic medium and proved to be inactive in the phenol/4-aminoantipyrine test (see Section 3.4.).

The mechanism shown in Scheme 4 summarizes kinetics and spectroscopic evidences for the peroxidatic activity of MnL^-, including the formation of the inactive oxo-bridged Mn(IV)Mn(IV) dimer.

4. Conclusions

The first oxidation products of glycerol are GA and DHA. Since GA resulted to be a bioactive molecule, this study further focused on its catalytic production over the already industrially produced DHA. Thus, glycerol oxidation trials were conducted and followed by aldehyde detection by means of the Schiff test. Gas chromatography of reaction product confirmed the presence of GA. Thus, under mild conditions and in the absence of organic solvents GA was produced as a sole reaction product. Nonetheless, glycerol conversion and GA production were low for both catalysts.

Superoxide to peroxy radicals ratio depends on medium pH. Both radicals may combine to generate dioxygen however they are also very active oxidizing agents themselves and are able to degrade organic matter, like glycerol molecule. In fact, we could confirm in Section 3.3 that Fenton treatment of glycerol solutions was effective. Aldehyde production kinetics in case of hematin (Fig. 1) showed initial rates equals to zero, which are consistent with a radical mechanism in a consecutive reaction pathway, in which GA is the product of the interaction of previously generated inorganic radical species with glycerol. Superoxide and or peroxy radicals are also involved in porphyrin degradation [38] which is manifested in our experiments with hematin as the bleaching. In a prior work, we demonstrated that dioxygen production from H_2O_2 catalyzed by hematin is lowered and in some cases completely suppressed in the presence of a reducing substrate like phenol [29]. As a matter of fact, reducing substrates act as a protecting agent against suicidal inactivation of horseradish peroxidase, whose hematin is its biomimetic structure [38]. Thus, glycerol may not be a proper substrate for hematin compound I and the marginal glycerol oxidation observed in hematin systems might be due to both, the direct action of generated superoxide to glycerol molecules or a Fenton mechanism triggered by liberated iron from porphyrin bleaching.

On the other hand, MnL^- presented poor catalytic properties for GA production from H_2O_2 treated glycerol solutions. Moreover, the catalatic as well as the peroxidatic activity of MnL^- showed a clear prompt decay with time. The addition of higher donor solvents like DMSO, DMF or acetone to the basic buffer system improved the peroxidatic activity due to promotion of Mn(IV) or Mn(V) formation. Finally, EPR spectroscopy of MnL supported the hypothesis of the formation of inactive bis-oxo-bridged Mn(IV)Mn(IV) dimer upon addition of H_2O_2 in DMSO, which is also favored in basic media as *e.g.* the buffer systems and mixtures of solvents tested in the peroxidatic and catalatic tests.

The influence of reaction media on H_2O_2, dioxygen and bleaching profile during glycerol – but also of phenolic substrates as a positive control - solutions treated with H_2O_2 in the presence and absence of both metal complexes will be the focus of forthcoming studies. Even a combination of hematin and MnL^- can be also promising, acting the last as a superoxide scavenger.

Acknowledgements

The authors thank the National University of Córdoba (Secyt project type A), the National University of Rosario and CONICET for the financial support (PIP 0337 and PIP 0941).

References

[1] S. Enthaler, K. Junge, M. Beller, Sustainable metal catalysis with iron: from rust to a rising star? Angew. Chem. Int. Ed. 47 (2008) 3317–3321, https://doi.org/10.1002/anie.200800012.
[2] C. Stopiglia, F. Vieira, A. Mondadori, T. Oppe, M. Scroferneker, In vitro antifungal activity of dihydroxyacetone against causative agents of dermatomycosis, Mycopathologia 171 (2011) 267–271, https://doi.org/10.1007/s11046-010-9370-x.
[3] B. Katryniok, H. Kimura, E. Skrzyńska, J.-S. Girardon, P. Fongarland, M. Capron, R. Ducoulombier, N. Mimura, S. Paul, F. Dumeignil, Selective catalytic oxidation of glycerol: perspectives for high value chemicals, Green Chem. 13 (2011) 1960, https://doi.org/10.1039/c1gc15320j.
[4] H.J. Dorman, S.G. Deans, Antimicrobial agents from plants: antibacterial activity of plant volatile oils, J. Appl. Microbiol. 88 (2000) 308–316.
[5] S.D. Rubbo, J.F. Gardner, R.L. Webb, Biocidal activities of glutaraldehyde and related compounds, J. Appl. Bacteriol. 30 (1967) 78–87.
[6] R.C. Gueldner, D.M. Wilson, A.R. Heidt, Volatile compounds inhibiting Aspergillus flavus, J. Agric. Food Chem. 33 (1985) 411–413, https://doi.org/10.1021/jf00063a022.
[7] I.H. Han, A.S. Csallany, Formation of toxic α,β-unsaturated 4-hydroxy-aldehydes in

thermally oxidized fatty acid methyl esters, J. Am. Oil Chem. Soc. 86 (2009) 253–260, https://doi.org/10.1007/s11746-008-1343-6.
[8] U. Stemmer, A. Hermetter, Protein modification by aldehydophospholipids and its functional consequences, Biochim. Biophys. Acta 1818 (2012) 2436–2445, https://doi.org/10.1016/j.bbamem.2012.03.006.
[9] Ramirez-Rodriguez Ramos-Nino, Adams Clifford, QSARs for the effect of benzaldehydes on foodborne bacteria and the role of sulfhydryl groups as targets of their antibacterial activity, J. Appl. Microbiol. 84 (2002) 207–212, https://doi.org/10.1046/j.1365-2672.1998.00324.x.
[10] S.E. Walsh, J.Y. Maillard, C. Simons, A.D. Russell, Studies on the mechanisms of the antibacterial action of ortho-phthalaldehyde, J. Appl. Microbiol. 87 (1999) 702–710.
[11] F. Testud, J. Descotes, J.B.T.-H.T. DESCOTES (Ed.), Aldehydes, Esters, Ketones, Ethers and Amines, Elsevier Science, B.V., Amsterdam, 1996, pp. 649–660, , https://doi.org/10.1016/B978-044481557-6/50027-7.
[12] S.R. Clough, Glyceraldehyde A2 - Wexler, Philip BT - Encyclopedia of Toxicology, second edition, Elsevier, New York, 2005, pp. 448–449, https://doi.org/10.1016/B0-12-369400-0/00456-7.
[13] P.K. Dikshit, S.K. Padhi, V.S. Moholkar, Process optimization and analysis of product inhibition kinetics of crude glycerol fermentation for 1,3-Dihydroxyacetone production, Bioresour. Technol. 244 (2017) 362–370, https://doi.org/10.1016/j.biortech.2017.07.136.
[14] A.C. Garcia, Y.Y. Birdja, G. Tremiliosi-Filho, M.T.M. Koper, Glycerol electro-oxidation on bismuth-modified platinum single crystals, J. Catal. 346 (2017) 117–124, https://doi.org/10.1016/j.jcat.2016.12.013.
[15] C.V. Piattoni, C.M. Figueroa, M.D. Asención Diez, I.L. Parcerisa, S. Antuña, R.A. Comelli, S.A. Guerrero, A.J. Beccaria, A.Á. Iglesias, Production and characterization of Escherichia coli glycerol dehydrogenase as a tool for glycerol recycling, Process Biochem. 48 (2013) 406–412, https://doi.org/10.1016/j.procbio.2013.01.011.
[16] J.C. Beltrán-Prieto, K. Kolomazník, J. Pecha, A review of catalytic systems for glycerol oxidation: alternatives for waste valorization, Aust. J. Chem. 66 (2013) 511–521, https://doi.org/10.1071/CH12514.
[17] E. Farnetti, C. Crotti, Selective oxidation of glycerol to formic acid catalyzed by iron salts, Catal. Commun. 84 (2016) 1–4, https://doi.org/10.1016/j.catcom.2016.05.014.
[18] E. Skrzyńska, S. Zaid, J.S. Girardon, M. Capron, F. Dumeignil, Catalytic behaviour of four different supported noble metals in the crude glycerol oxidation, Appl. Catal. A Gen. (2015), https://doi.org/10.1016/j.apcata.2015.04.008.
[19] Aa. Rodriguez, C.T. Williams, J.R. Monnier, Selective liquid-phase oxidation of glycerol over Au–Pd/C bimetallic catalysts prepared by electroless deposition, Appl. Catal. A Gen. 475 (2014) 161–168, https://doi.org/10.1016/j.apcata.2014.01.011.
[20] A. Villa, N. Dimitratos, C.E. Chan-Thaw, C. Hammond, L. Prati, G.J. Hutchings, Glycerol oxidation using gold-containing catalysts, Acc. Chem. Res. (2015), https://doi.org/10.1021/ar500426g.
[21] E.G. Rodrigues, S.A.C. Carabineiro, X. Chen, J.J. Delgado, J.L. Figueiredo, M.F.R. Pereira, J.J.M. Órfão, Selective oxidation of glycerol catalyzed by Rh/activated carbon: importance of support surface chemistry, Catal. Lett. (2011), https://doi.org/10.1007/s10562-010-0515-9.
[22] S. Gil, M. Marchena, C.M. Fernández, L. Sánchez-Silva, A. Romero, J.L. Valverde, Catalytic oxidation of crude glycerol using catalysts based on Au supported on carbonaceous materials, Appl. Catal. A Gen. 450 (2013) 189–203, https://doi.org/10.1016/j.apcata.2012.10.024.
[23] S. Hirasawa, H. Watanabe, T. Kizuka, Y. Nakagawa, K. Tomishige, Performance, structure and mechanism of Pd-Ag alloy catalyst for selective oxidation of glycerol to dihydroxyacetone, J. Catal. 300 (2013) 205–216, https://doi.org/10.1016/j.jcat.2013.01.014.
[24] R.A. Sheldon, Catalytic oxidations in the manufacture of fine chemicals, Stud. Surf. Sci. Catal. (1990), https://doi.org/10.1016/S0167-2991(08)60130-5.
[25] R. Noyori, M. Aoki, K. Sato, Green oxidation with aqueous hydrogen peroxide, Chem. Commun. (Camb) (2003), https://doi.org/10.5363/tits.14.3_60.
[26] P. Gallezot, Selective oxidation with air on metal catalysts, Catal. Today (1997), https://doi.org/10.1016/S0920-5861(97)00024-2.
[27] C.M. Che, J.S. Huang, Metalloporphyrin-based oxidation systems: from biomimetic reactions to application in organic synthesis, Chem. Commun. (2009), https://doi.org/10.1039/b901221d.
[28] P.E. Ellis, J.E. Lyons, Selective air oxidation of light alkanes catalyzed by activated metalloporphyrins - the search for a suprabiotic system, Coord. Chem. Rev. (1990), https://doi.org/10.1016/0010-8545(90)80022-L.
[29] H. Hosseini-Monfared, C. Näther, H. Winkler, C. Janiak, Highly selective and “green” alcohol oxidations in water using aqueous 10% H2O2and iron-benzene-tricarboxylate metal-organic gel, Inorganica Chim. Acta (2012), https://doi.org/10.1016/j.ica.2012.05.007.
[30] R.R. Fernandes, J. Lasri, M.F.C. Guedes Da Silva, J.A.L. Da Silva, J.J.R. Fraústo Da Silva, A.J.L. Pombeiro, Bis- and tris-pyridyl amino and imino thioether Cu and Fe complexes. Thermal and microwave-assisted peroxidative oxidations of 1-phenylethanol and cyclohexane in the presence of various N-based additives, J. Mol. Catal. A Chem. (2011), https://doi.org/10.1016/j.molcata.2011.09.022.
[31] S.A. Moyer, T.W. Funk, Air-stable iron catalyst for the Oppenauer-type oxidation of alcohols, Tetrahedron Lett. (2010), https://doi.org/10.1016/j.tetlet.2010.08.004.
[32] C. Crotti, E. Farnetti, Selective oxidation of glycerol catalyzed by iron complexes, J. Mol. Catal. A Chem. 396 (2015) 353–359, https://doi.org/10.1016/j.molcata.2014.10.021.
[33] T.L. Poulos, Thirty years of heme peroxidase structural biology, Arch. Biochem. Biophys. 500 (2010) 3–12, https://doi.org/10.1016/j.abb.2010.02.008.
[34] G. Battistuzzi, M. Bellei, C.A. Bortolotti, M. Sola, Redox properties of heme peroxidases, Arch. Biochem. Biophys. 500 (2010) 21–36, https://doi.org/10.1016/j.abb.2010.03.002.
[35] A. Córdoba, I. Magario, M.L. Ferreira, Evaluation of hematin-catalyzed Orange II degradation as a potential alternative to horseradish peroxidase, Int. Biodeterior. Biodegrad. 73 (2012) 60–72, https://doi.org/10.1016/j.ibiod.2012.05.020.
[36] A. Córdoba, I. Magario, M.L. Ferreira, Experimental design and MM2–PM6 molecular modelling of hematin as a peroxidase-like catalyst in Alizarin Red S degradation, J. Mol. Catal. A Chem. 355 (2012) 44–60, https://doi.org/10.1016/J.MOLCATA.2011.12.011.
[37] M. Rong, J. Wang, Y. Shen, J. Han, Catalytic oxidation of alcohols by a novel manganese Schiff base ligand derived from salicylaldehyd and l-Phenylalanine in ionic liquids, Catal. Commun. 20 (2012) 51–53, https://doi.org/10.1016/j.catcom.2011.11.035.
[38] W. Al Zoubi, Y.G. Ko, Organometallic complexes of Schiff bases: recent progress in oxidation catalysis, J. Organomet. Chem. 822 (2016) 173–188, https://doi.org/10.1016/j.jorganchem.2016.08.023.
[39] K.C. Gupta, A.K. Sutar, Catalytic activities of Schiff base transition metal complexes, Coord. Chem. Rev. (2008), https://doi.org/10.1016/j.ccr.2007.09.005.
[40] K.C. Gupta, A. Kumar Sutar, C.-C. Lin, Polymer-supported Schiff base complexes in oxidation reactions, Coord. Chem. Rev. (2009), https://doi.org/10.1016/j.ccr.2009.03.019.
[41] B. Bahramian, V. Mirkhani, M. Moghadam, A.H. Amin, Water-soluble manganese (III) salen complex as a mild and selective catalyst for oxidation of alcohols, Appl. Catal. A Gen. 315 (2006) 52–57, https://doi.org/10.1016/j.apcata.2006.08.037.
[42] M.K. Brown, M.M. Blewett, J.R. Colombe, E.J. Corey, Mechanism of the enantioselective oxidation of racemic secondary alcohols catalyzed by chiral Mn (III) − Salen complexes, J. Am. Chem. Soc. 132 (2010) 11165–11170, https://doi.org/10.1021/ja103103d.
[43] D. Xu, S. Wang, Z. Shen, C. Xia, W. Sun, Enantioselective oxidation of racemic secondary alcohols catalyzed by chiral Mn(iii)-salen complexes with N-bromosuccinimide as a powerful oxidant, Org. Biomol. Chem. 10 (2012) 2730–2732, https://doi.org/10.1039/C2OB07087A.
[44] V.K. Bansal, R. Kumar, R. Prasad, S. Prasad, Niraj, Catalytic chemical and electrochemical wet oxidation of phenol using new copper(II) tetraazamacrocycle complexes under homogeneous conditions, J. Mol. Catal. A Chem. 284 (2008) 69–76, https://doi.org/10.1016/j.molcata.2007.12.030.
[45] É. Balogh-Hergovich, G. Speier, Catalytic oxidation of alcohols to carbonyl compounds with hydrogen peroxide using dinuclear iron complexes, J. Mol. Catal. A Chem. 230 (2005) 79–83, https://doi.org/10.1016/j.molcata.2004.12.013.
[46] A. Córdoba, N. Alasino, M. Asteasuain, I. Magario, M.L. Ferreira, Mechanistic evaluation of hematin action as a horseradish peroxidase biomimetic on the 4-aminoantipyrine/phenol oxidation reaction, Chem. Eng. Sci. 129 (2015) 249–259, https://doi.org/10.1016/j.ces.2015.02.031.
[47] D. Moreno, V. Daier, C. Palopoli, J.-P. Tuchagues, S. Signorella, Synthesis, characterization and antioxidant activity of water soluble MnIII complexes of sulphonato-substituted Schiff base ligands, J. Inorg. Biochem. 104 (2010) 496–502, https://doi.org/10.1016/j.jinorgbio.2009.12.016.
[48] C.M. Mann, J.L. Markham, A new method for determining the minimum inhibitory concentration of essential oils, J. Appl. Microbiol. 84 (1998) 538–544.
[49] Farmacopedia Argentina, Ministry of Health of The Nation, 7th edition, (2003).
[50] T. Kajiwara, K. Matsui, Y. Akakabe, T. Murakawa, C. Arai, Antimicrobial browning-inhibitory effect of flavor compounds in seaweeds, J. Appl. Phycol. 18 (2006) 413–422, https://doi.org/10.1007/s10811-006-9046-6.
[51] J.C. Matasyoh, Z.C. Maiyo, R.M. Ngure, R. Chepkorir, Chemical composition and antimicrobial activity of the essential oil of Coriandrum sativum, Food Chem. 113 (2009) 526–529, https://doi.org/10.1016/j.foodchem.2008.07.097.
[52] G.M. N, O. M, C. C, D. J, L. A, Z. J, D. M, Antimicrobial combined action of terpenes against the food-borne microorganisms Escherichia coli, Staphylococcus aureus and Bacillus cereus, Flavour Fragr. J. 24 (2009) 348–354, https://doi.org/10.1002/ffj.1948.
[53] S. Dosler, E. Karaaslan, Inhibition and destruction of Pseudomonas aeruginosa biofilms by antibiotics and antimicrobial peptides, Peptides 62 (2014) 32–37, https://doi.org/10.1016/j.peptides.2014.09.021.
[54] W.D. Nicoll, A.F. Smith, Stability of dilute alkaline solutions of hydrogen peroxide, Ind. Eng. Chem. 47 (1955) 2548–2554, https://doi.org/10.1021/ie50552a051.
[55] G. Wu, X. Wang, T. Jiang, Q. Lin, Selective oxidation of glycerol with 3% H2O2 catalyzed by LDH-Hosted Cr(III) complex, Catalysts (2015), https://doi.org/10.3390/catal5042039.
[56] J. Luo, H. Li, N. Zhao, F. Wang, F. Xiao, Selective oxidation of glycerol to dihydroxyacetone over layer double hydroxide intercalated with sulfonato-salen metal complexes, J. Fuel Chem. Technol. 43 (2015) 677–683, https://doi.org/10.1016/S1872-5813(15)30019-0.
[57] R. Azadbakht, A. Amini Manesh, M. Malayeri, B. Dehghani, Synthesis, characterization, reactivity and catalytic activity of a novel chiral manganese Schiff base complex, New J. Chem. (2015), https://doi.org/10.1039/c5nj01031d.
[58] G.B. Shul’Pin, Y.N. Kozlov, L.S. Shul’Pina, T.V. Strelkova, D. Mandelli, Oxidation of reactive alcohols with hydrogen peroxide catalyzed by manganese complexes, Catal. Lett. 138 (2010) 193–204, https://doi.org/10.1007/s10562-010-0398-9.
[59] I. Magario, F.S. García Einschlag, E.H. Rueda, J. Zygadlo, M.L. Ferreira, Mechanisms of radical generation in the removal of phenol derivatives and pigments using different Fe-based catalytic systems, J. Mol. Catal. A Chem. 352 (2012) 1–20, https://doi.org/10.1016/j.molcata.2011.10.006.
[60] I. Magario, A. Neumann, E. Oliveros, C. Syldatk, Deactivation kinetics and response surface analysis of the stability of alpha-L-rhamnosidase from Penicillium decumbens, Appl. Biochem. Biotechnol. 152 (2009) 29–41.
[61] S. Signorella, C. Palopoli, G. Ledesma, Rationally designed mimics of antioxidant

manganoenzymes: role of structural features in the quest for catalysts with catalase and superoxide dismutase activity, (2018), https://doi.org/10.1016/j.ccr.2018.03.005.
[62] C. Cabrera, A. Cornaglia, A. Córdoba, I. Magario, M.L. Ferreira, Kinetic modelling of the hematin catalysed decolourization of Orange II solutions, Chem. Eng. Sci. 161 (2017) 127–137, https://doi.org/10.1016/j.ces.2016.11.049.
[63] T. Kurahashi, Reverse catalase reaction: dioxygen activation via two-electron transfer from hydroxide to dioxygen mediated by a manganese(III) salen complex, Inorg. Chem. 54 (2015) 8356–8366, https://doi.org/10.1021/acs.inorgchem.5b01025.
[64] J. Zhang, Y. Tang, J.Q. Xie, J.Z. Li, W. Zeng, C.W. Hu, Study on phenol oxidation with H2O2catalyzed by Schiff base manganese complexes as mimetic peroxidase, J. Serbian Chem. Soc. (2005), https://doi.org/10.2298/JSC05101137Z.
[65] X.G. Meng, J. Zhu, J. Yan, J.Q. Xie, X.M. Kou, X.F. Kuang, L.F. Yu, X.C. Zeng, Studies on the oxidation of phenols catalyzed by a copper(II)-Schiff base complex in aqueous solution under mild conditions, J. Chem. Technol. Biotechnol. 81 (2006) 2–7, https://doi.org/10.1002/jctb.1349.
[66] A. Panja, N.C. Jana, P. Brandão, Influence of anions and solvents on distinct coordination chemistry of cobalt and effect of coordination spheres on the biomimetic oxidation of o-aminophenols, Mol. Catal. (2018), https://doi.org/10.1016/j.mcat.2018.02.013.
[67] S.F. Mapolie, J.L. Van Wyk, Synthesis and characterization of dendritic salicylaldimine complexes of copper and cobalt and their use as catalyst precursors in the aerobic hydroxylation of phenol, Inorg. Chim. Acta (2013), https://doi.org/10.1016/j.ica.2012.09.006.
[68] K.C. Gupta, A.K. Sutar, Catalytic activity of polymer anchored N,N′-bis (o-hydroxy acetophenone) ethylene diamine Schiff base complexes of Fe(III), Cu(II) and Zn(II) ions in oxidation of phenol, React. Funct. Polym. (2008), https://doi.org/10.1016/j.reactfunctpolym.2007.10.015.
[69] K.C. Gupta, A.K. Sutar, Polymer anchored Schiff base complexes of transition metal ions and their catalytic activities in oxidation of phenol, J. Mol. Catal. A Chem. (2007), https://doi.org/10.1016/j.molcata.2007.03.025.
[70] W. Hu, J.Z. Li, Y. Wang, J. Du, C.W. Hu, X.C. Zeng, Studies on phenol oxidation with h2o2catalyzed by schiff base cobalt(ii) complexes in micellar solution, J. Dispers. Sci. Technol. (2008), https://doi.org/10.1080/01932690802313667.
[71] J.L. van Wyk, S.F. Mapolie, A. Lennartson, M. Håkansson, S. Jagner, The catalytic oxidation of phenol in aqueous media using cobalt(II) complexes derived from N-(aryl) salicylaldimines, Inorganica Chim. Acta (2008), https://doi.org/10.1016/j.ica.2007.10.031.
[72] J.W. Gohdes, W.H. Armstrong, Synthesis, structure, and properties of [Mn(salpn)(EtOH)2](ClO4) and its aerobic oxidation product [Mn(salpn)O]2, Inorg. Chem. 31 (1992) 368–373, https://doi.org/10.1021/ic00029a007.
[73] P. Ratnasamy, D. Srinivas, H.B.T. Knözinger, Active sites and reactive intermediates in titanium silicate molecular sieves, Adv. Catal. Academic Press, 2004, pp. 1–169, https://doi.org/10.1016/S0360-0564(04)48001-8.
[74] B.A. Goodman, J.B. Raynor, H.J. Emeléus, A.G.B.T.-A, I.C, R. Sharpe (Eds.), Electron Spin Resonance of Transition Metal Complexes, Academic Press, 1970, pp. 135–362, , https://doi.org/10.1016/S0065-2792(08)60336-2.
[75] A. Bencini, D. Gatteschi, Electron Paramagnetic Resonance of Exchange Coupled Systems, 1st ed., Springer-Verlag, Berlin Heidelberg, 1990, https://doi.org/10.1007/978-3-642-74599-7.